FINITE ELEMENT ANALYSIS OF BONDED JOINTS IN COMPOSITE MATERIALS

M. Quaresimin and M. Ricotta

Department of Management and Engineering, University of Padova, Stradella San Nicola 3, Vicenza, 36100, Italy

ABSTRACT

The paper presents the results of several numerical analyses carried out with aim to investigate the stress fields and simulate crack propagation in composite joints, thus providing tools for the development of life prediction methodologies. Single lap bonded joints with different overlap length and corner geometry were studied. In view of predicting static strength and fatigue crack initiation, stress distributions and generalised stress intensity factors near the singular zones were evaluated on un-cracked FE models by geometrically linear analyses. For simulating the crack growth, the Strain Energy Release Rate trends as a function of the crack length were estimated by using Virtual Crack Closure Technique. In this case, results obtained from geometrically linear and non-linear analyses are compared, being the latter those providing more reliable results.

1. INTRODUCTION

The availability of adhesives with high performances and relatively low cost could make bonded joints a valid alternative to riveted and bolted connections in many situations of practical interest in structural engineering, especially in composite material components. Hence, the development of reliable design tools for the prediction of strength and fatigue life of composite connections has been considered for a long time by the scientific community (see refs. [1-6] for some examples).

A stress intensity factor (SIF) approach has been extensively used to predict static strength in bonded joints since stress singularity arises, also in the absence of any geometrical discontinuity, due to the mismatch of the elastic properties of the connected materials [7].

Less frequent, instead, is the use of a generalised SIF approach to evaluate the fatigue strength of the joints. Lefebvre and Dillard [8] have proposed a stress intensity factor approach to predict the fatigue crack initiation in epoxy–aluminium wedge specimens. Imanaka and co-authors [9], in order to consider the stress singularity at the corners of the adhesive/adherent interface, based the fatigue life estimation on two "apparent" values for stress intensity factor and degree of singularity of the stress field in the critical zone of the joint.

On the assumption that the fatigue life of a bonded connection is dominated by the growth of a crack, many authors suggest a Strain Energy Release Rate (SEER) approach for the assessment of the fatigue life. It is worth noting however that, being the stress singularity degree no longer '-0.5', the connection between generalized intensity factor H and the SERR disappears [10]. Pradhan and co-authors [11] analysed adhesive-bonded joints using finite element method by computing SERR for debonding and suggested material properties and geometries to extend the load-carrying capability of joints. Wahab and co-authors [12] used the SERR to predict the fatigue threshold of double-lap and lap-strap joints. Kayupov and Dzenis [13] used non-linear finite element analysis to study stress fields in single-lap bonded joints. A near-linear dependence was observed between stress-intensity factors and the load levels for cracks with constant length, while a non linear dependence was observed between SERR and applied load values.

An extensive experimental activity, carried out by the authors in parallel to the analyses here presented, proved that the fatigue life of bonded joints in composite materials can be divided into two distinct phases: an initiation or nucleation phase followed by the crack growth up to a critical length. The fraction of the life spent in the two phases depends on many parameters like joint geometry, stress distributions, stress ratio, adhesive type and thickness, environmental conditions and others. The fatigue cracks nucleate and grow mainly in the adhesive or at the adhesive/adherend interface.

It is the authors' opinion that the more precise way to describe and model the fatigue life of a bonded joint is that which accounts for the actual evolution of the damage: an initiation or nucleation phase followed by a crack growth. In adhesive joints a crack usually nucleates and grows mainly in the adhesive or at the adhesive/adherent interface and therefore the life to crack initiation can be estimated using a generalised stress intensity factor approach. The duration of the propagation phase can be later assessed by integrating a suitable power law relating the crack growth rate to the strain energy release rate.
The paper presents the results of several two-dimensional Finite Element analyses carried out with the aim to investigate the stress fields in single lap bonded composite joints under tension, evaluating SIF and SERR as a function of the crack length. An uncracked FE model and geometrically linear analysis were adopted to evaluate the generalised stress intensity factor; on the other hand, the crack propagation was assumed to be at adherend-adhesive interface and the results of geometrically linear and non-linear analyses were compared for the SERR estimation. The numerical results presented here will be later integrated with the experimental results for the development of a suitable life prediction tools.

2. MATERIALS AND GEOMETRY OF JOINTS

The geometry of the joints under investigation is shown in Fig. 1: adhesive and adherend thickness are 0.15 mm and 1.65 mm, respectively. Two geometry corners were analysed: with (A) and without fillet (B). The joints were manufactured starting from a carbon/epoxy prepreg (T300 twill 2x2 fabric/toughened ET442) and were bonded with 3M 9323 B/A epoxy adhesive. Three overlap lengths (20, 30 and 40 mm) were investigated by keeping constant specimen width (25 mm) and overall length (260 mm), being the laminate lay-up $[0]_6$.
The elastic properties of the laminates to be used later for the numerical analyses are summarized in Table 1. The adherend's elastic properties were experimentally measured [14] and the adhesive properties were taken from commercial data sheet.

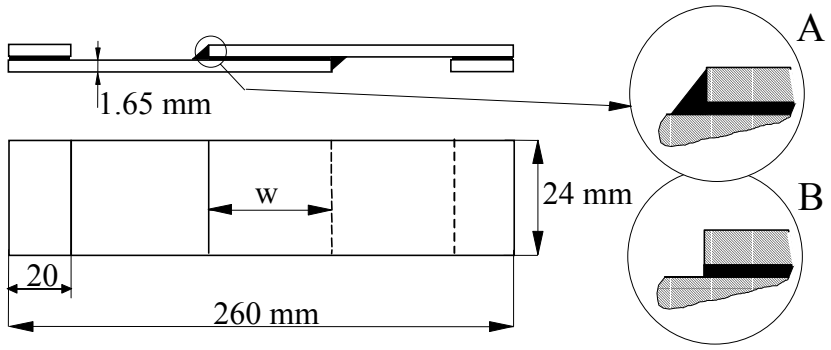

"**Fig. 1.** Geometry of single lap bonded joint."

"**Table 1.** Material properties of adherend and adhesive"

	E_L [MPa]	E_Y [MPa]	G_{LY} [MPa]	ν_{LY}
Adherend	58050	6000	500	0.27
Adhesive	2870	2870	1070	0.37

3. STRESS DISTRIBUTIONS AND FIELD PARAMETERS

As suggested in ref. [15], the stress distributions near the singularity of bonded joints can be described by a two-term stress expansion, under the hypothesis that both the first and the second terms are in the variable separable form. Each term can therefore be represented by a radial component with unknown exponent (eigenvalue) and an angular function, also unknown. The resulting analytical formulation of the stress distributions can be given as:

$$\sigma_{ij}(r,\theta) = H_0 r^s f^{(0)}{}_{ij}(\theta) + H_1 r^t f(\theta)^{(1)}{}_{ij} + ... \quad (1)$$

where the eingevalues s and t depend on corner geometry and elastic properties of the materials. In Eq. 1 the exponent s is to be thought of as negative to give a singular stress field and, moreover, it is stated for hypothesis that $s < t$. For linear elastic isotropic materials bonded together, the stress fields can be evaluated by the analytical method described in [15]. For joints made with anisotropic composite laminates, an analytical framework has not yet developed, hence the stress fields were obtained through finite element analysis.

2D finite element models of the joints were developed by using the Ansys 7.0® code and PLANE82 elements under plane strain conditions. In order to capture the asymptotic stress distribution near the singularity very fine meshes were adopted, by using the KSCON command of the ANSYS software, which is particularly useful for creating a fracture model around a singularity point. The total number of elements in the models, ranging from 5000 to 28000, depends on overlap length and presence of adhesive fillet being the smallest size element equal to 10^{-5} mm. Examples of the meshes near the singularity are shown in Fig. 2.

For the evaluation of stress fields and relevant generalised stress intensity factors H_0, an uncracked adhesive-adherend interface was modelled and an elastic and geometrically linear behaviour was assumed, according also to the results presented in [13]. This choice is also supported by some preliminary analyses which demonstrated that including the geometrical non linearity leads to some changes in stress fields but has negligible influence on the generalised stress intensity factor. The possible material non-linearity due to the adhesive was also neglected since dedicated experimental tensile tests and microscopic observations proved a brittle behaviour of the adhesive up to failure.

The stress distributions for different overlap length, different geometry of corner (with and without fillet) and two θ directions, are plotted in polar co-ordinates in Figs. 4-7 as a function of the distance from notch tip and according to the frame of reference shown in Fig. 3.

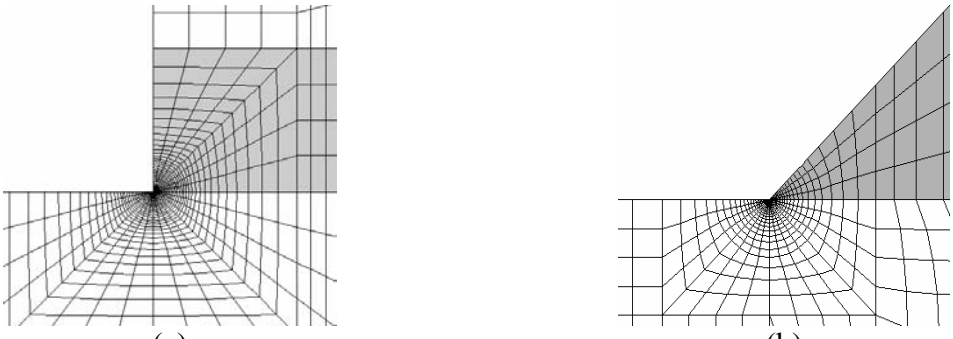

(a) (b)

"**Fig. 2.** Mesh of the joint near the singular zone for (a) square edge and (b) fillet tip"

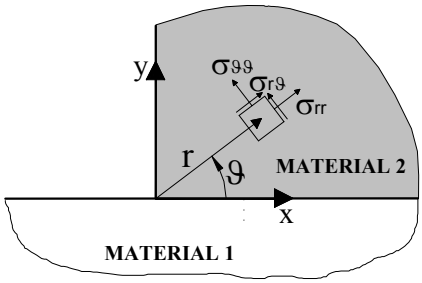

"**Fig. 3.** Schematic view of the singular zone showing the polar co-ordinate system."

The results confirm that in the close neighbourhood of the singularity points (r which tends towards zero), the first term of the stress distribution (see Eq. 1) becomes dominant and therefore the stress fields can be described by the following relationship:

$$\sigma_{ij}(r,\theta) = H_0 r^s f^{(0)}{}_{ij}(\theta) \tag{2}$$

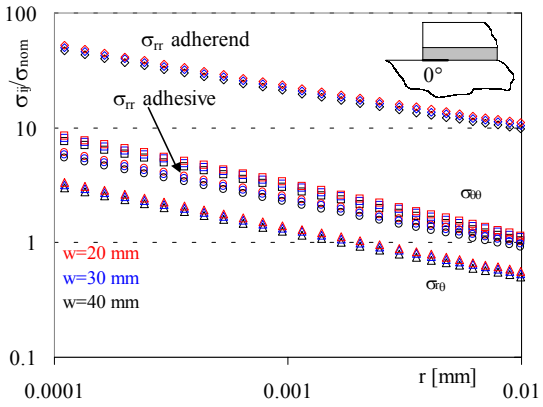

"**Fig. 4**. Normalised stress distributions for square-edge joint under tensile loading at θ=0°."

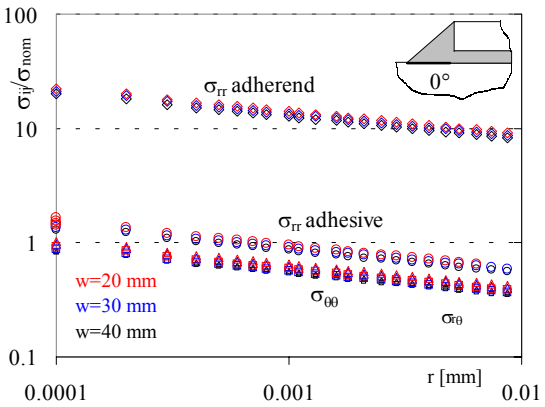

"**Fig. 5**. Normalised stress distributions for fillet joint under tensile loading at θ=0°."

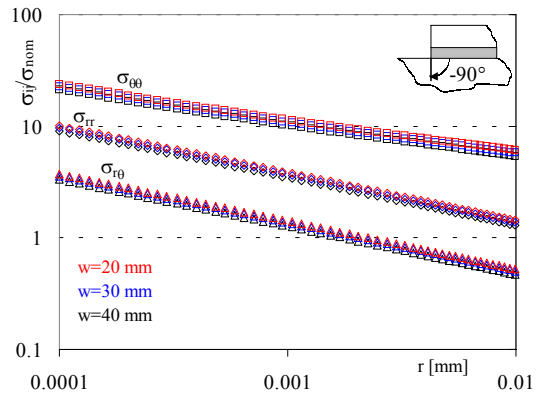

"**Fig. 6**. Normalised stress distributions for square-edge joint under tensile loading at θ=-90°."

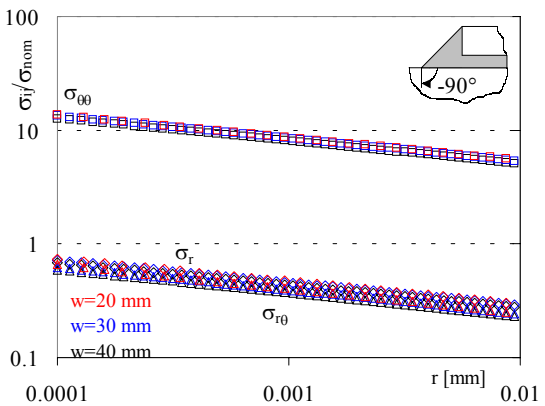

"**Fig. 7**. Normalised stress distributions for fillet joint under tensile loading at θ=-90°."

Table 2 and Table 3 summarise the eigenvalue s and the angular stress distribution functions $f^{(0)}_{ij}(\theta)$ (normalised assuming $f^{(0)}_{\theta\theta}(0)=1$) calculated in the adherend, for square-edge joint and fillet joint, respectively.

"**Table 2.** Eigenvalue s and angular stress distribution functions $f^{(0)}_{ij}(\theta)$ (normalised assuming $f^{(0)}_{\theta\theta}(0)=1$) calculated in the adherend, for square-edge joint."

w [mm]	s	$f^{(0)}_{\theta\theta}(\theta)$ (θ=0°)	$f^{(0)}_{rr}(\theta)$ (θ=0°)	$f^{(0)}_{r\theta}(\theta)$ (θ=0°)	$f^{(0)}_{\theta\theta}(\theta)$ (θ=–90°)	$f^{(0)}_{rr}(\theta)$ (θ=–90°)	$f^{(0)}_{r\theta}(\theta)$ (θ=–90°)
20	-0.3440	1	12.7160	0.5804	7.5935	1.3188	0.4748
30	-0.3440	1	12.5168	0.5755	7.4342	1.3135	0.4729
40	-0.3440	1	12.5681	0.5446	7.4748	1.3151	0.4734

"**Table 3.** Eigenvalue s and angular stress distribution functions $f^{(0)}_{ij}(\theta)$ (normalised assuming $f^{(0)}_{\theta\theta}(0)=1$) calculated in the adherend, for fillet joint."

w [mm]	s	$f^{(0)}_{\theta\theta}(\theta)$ (θ=0°)	$f^{(0)}_{rr}(\theta)$ (θ=0°)	$f^{(0)}_{r\theta}(\theta)$ (θ=0°)	$f^{(0)}_{\theta\theta}(\theta)$ (θ=–90°)	$f^{(0)}_{rr}(\theta)$ (θ=–90°)	$f^{(0)}_{r\theta}(\theta)$ (θ=–90°)
20	-0.2010	1	24.8576	1.0796	15.8724	0.8689	0.6765
30	-0.2010	1	24.1400	1.0909	15.3052	0.8398	0.6494
40	-0.2010	1	24.2662	1.0923	15.5154	0.8338	0.6546

"**Table 4.** Generalised stress intensity factors H_0 "

	Square-edge	Fillet
w [mm]	H_0 [MPa mm^{-s}]	H_0 [MPa mm^{-s}]
20	0.1609	0.1419
30	0.1550	0.1386
40	0.1447	0.1300

Table 4 summarises the generalised stress intensity factor H_0 obtained, for all overlap lengths and both geometry corners, from linear FE analyses by simulating a nominal tensile stress equal to 1MPa. The values of generalised stress intensity factor H_0, for the same geometry corner, decrease as the overlap length increases, as already found for isotropic adherend [15]; moreover, the fillet presence reduces both the absolute value of eigenvalue s and the generalised stress intensity factor H_0, for the same overlap length, justifying the better performances of fillet joints experimentally observed in ref. [16].

4. STRAIN ENERGY RELEASE RATE

As already discussed in the introduction, a parameter frequently used to describe the crack propagation is the Strain Energy Release Rate (SERR), **G**. Since in the single lap joints the crack propagation is often a mixed mode fracture process, in a two-dimensional problem, the

total Strain Energy Release Rate G_{tot} can be subdivided into a Mode I component G_I and a Mode II component G_{II}: the Virtual Crack Closure Technique (VCCT) allows to separate the two components [17, 18]. To evaluate the SERR components, the approach suggested in Ref. [19], which accounts for the actual deformed shape of the joints, was used. The formulations, based on the nodal forces and displacements at the crack tip as described in Fig. 8, are reported in Eq. 3 and Eq. 4.

$$G_I = -\frac{1}{2\Delta a}\left[F_{\eta,i}\left(U_{\eta,l} - U'_{\eta,l}\right) + F_{\eta,j}\left(U_{\eta,m} - U'_{\eta,m}\right)\right] \tag{3}$$

$$G_{II} = -\frac{1}{2\Delta a}\left[F_{\xi,i}\left(U_{\xi,l} - U'_{\xi,l}\right) + F_{\xi,j}\left(U_{\xi,m} - U'_{\xi,m}\right)\right] \tag{4}$$

2D finite element models of the joints were developed again by using PLANE82 elements under plane strain conditions; however, as required by VCCT, a different meshing strategy was adopted, modelling the region near the crack tip with regular shape elements of uniform size. As a preliminary activity, a sensitivity analysis was carried out for the definition of a suitable element size. This analysis was carried out for a joint with overlap length (20 mm), crack length (5 mm), applied load (1 MPa) and different element size for the elements near the crack tip and the results are shown in Fig. 9. On this basis, the size of the smallest element was chosen equal to 30 μm for all the following analyses.

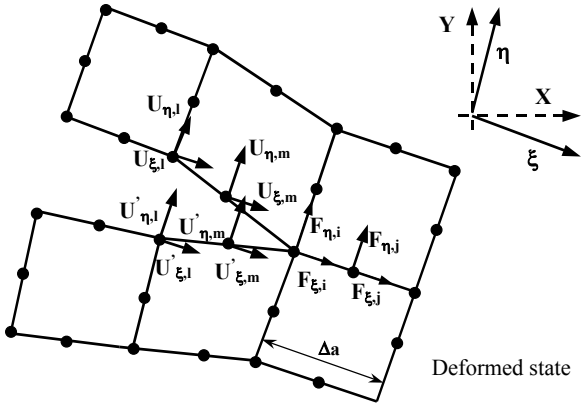

"**Fig. 8.** Nodal forces and displacements at the crack tip for applying VCCT in non-linear analysis"

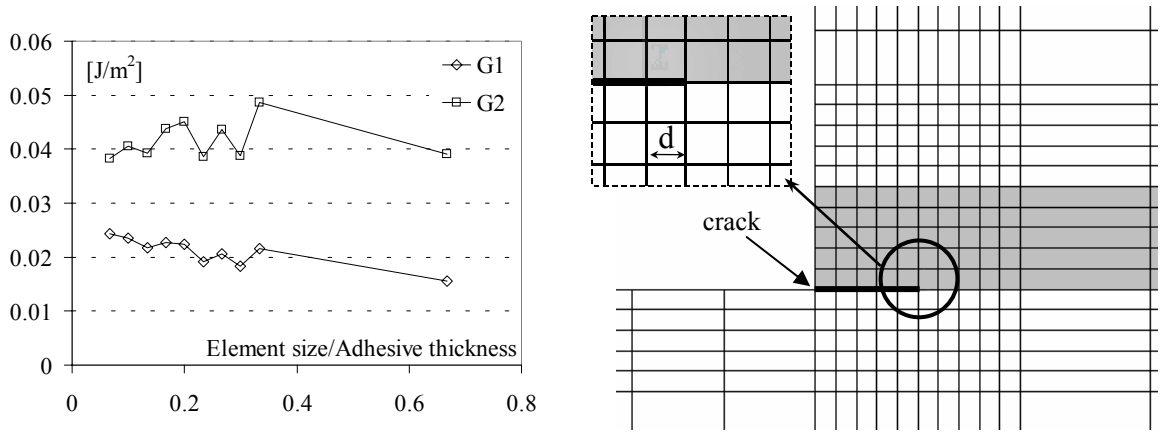

"**Fig. 9.** Element size effect in SERR evaluation"

The FE analyses were carried out under the alternative hypothesis of small and large displacements (geometrically linear and non-linear analyses) and the relevant results were compared and discussed. Dedicated experimental results indicated, however, the geometrically non-linear analyses as the more suitable approach to capture the effects of the out-of-plane bending in the joints.

Figs. 10 and 11 compare the results obtained for square-edge corner joints and two overlap length in the case of linear and non-linear analysis. The applied nominal tensile stress σ_{nom} corresponds, in both cases, to the relevant high cycle fatigue strength, taken from Ref. [16]. For an easier comparison of the results related to joints with different overlap, the SERR values are plotted as a function of normalised crack length. The linear analyses provide greater values for mode II component and lower for mode I component, confirming the lower accuracy in the out-of-plane displacements evaluation.

The two approaches are compared also in terms of total SERR in Figs. 12 and 13, where the trends for two stress levels are reported. High cycle fatigue strength is again considered as a first stress level together with the stress inducing a medium fatigue life (about 50.000 cycles). The linear analyses provide always greater SERR values. Moreover, as one could have expected, the difference between the two approaches becomes more significant at the higher stress levels.

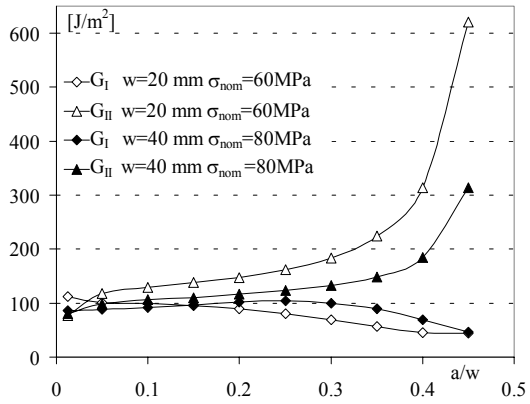

"**Fig. 10.** SERR Mode I and mode II components G_I and G_{II} evaluated by linear analysis"

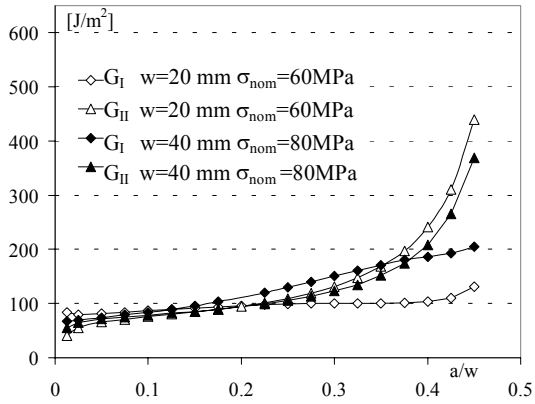

"**Fig. 11.** SERR Mode I and mode II components G_I and G_{II} evaluated by non-linear analysis"

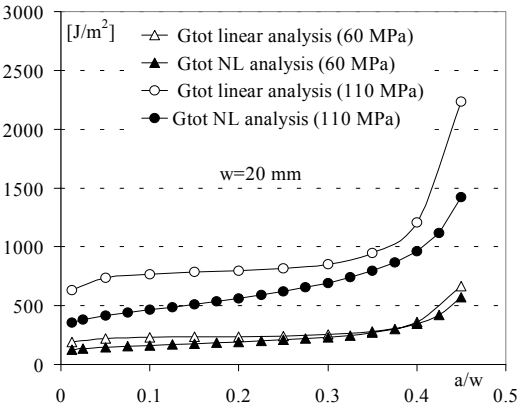

"**Fig. 12.** Influence of the stress level on G_{tot} evaluated using linear and non-linear analysis (w=20 mm)"

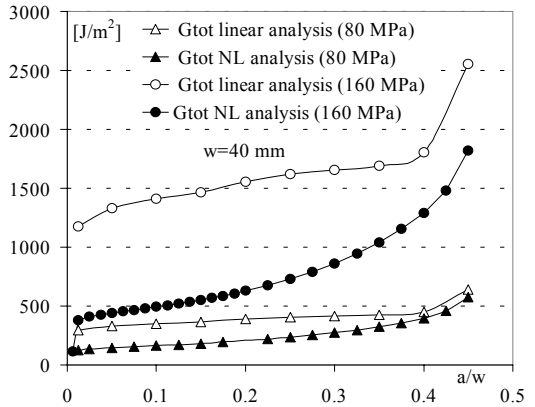

"**Fig. 13.** Influence of the stress level on G_{tot} evaluated using linear and non-linear analysis (w=40 mm)"

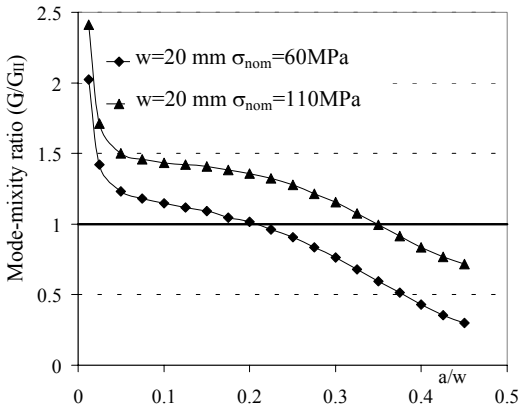

"**Fig. 14.** Influence of the stress level on mode-mixity ratio (w=20 mm, from non-linear FE analysis)"

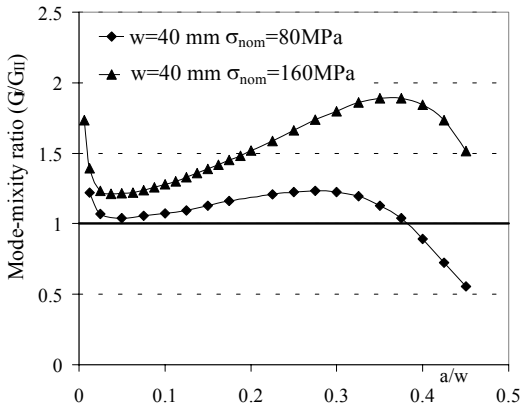

"**Fig. 15.** Influence of the stress level on mode-mixity ratio (w=40 mm, from non-linear FE analysis)"

Figs. 14 and 15 show the trends of mode mixity ratios obtained from the non-linear analyses. It can be easily seen that, for both the overlap lengths, the contribution of the Mode I component becomes more important as the applied stress increases. By comparing the two figures, the influence of the overlap length on the joint behaviour can be observed. For the shorter overlap at low stress level the mode mixity-ratio drops below unity for short crack lengths. On the other hand, in all the remaining cases, the mixity-ratio is well greater than unity indicating that the fracture process could be probably controlled by Mode I component.

5. CONCLUSIONS

Single lap bonded composite joints of different geometry were numerically analysed. Generalised stress intensity factors H_0 and Strain Energy Release Rate as a function of the crack length were evaluated.

The main results can be summarised as follows:

- As found for bonded joints made of isotropic materials, the H_0 value decreases as the overlap length increases. Moreover, the presence of fillet reduces both the absolute value of singularity and the H_0 value.
- Significant differences in the SERR evaluation, particularly at the higher stress levels, were found by comparing the results of geometrically linear and non-linear analyses, the former always providing greater values of the total SERR. A further comparison with experimental results, in terms of out-of-plane displacements, demonstrated however the greater reliability and accuracy for the non-linear analyses.
- As the overlap and the applied stress increase the mode I component of the SERR becomes dominant suggesting it as the driving force of the fracture process.

References

1. **Kinloch A. J.** and **Osiyemi S. O.,** "Predicting the fatigue life of adhesively-bonded joints", *J of Adhesion*, **43**, (1993), 79-90.
2. **Nayeb-Hashemi H., Rossettos J. N.,** and **Melo A. P.**, "Multiaxial fatigue life evaluation of tubular adhesively bonded joints", *Int J Adhes Adhes*, (1997), **17**, 55-63.
3. **Ishii K., Imanaka M., Nakayama H.,** and **Kodama H.**, "Fatigue failure criterion of adhesively bonded CFRP/metal joints under multiaxial stress conditions", *Compos part a-appl s*, (1998), **29**/A, 415-422.
4. **Ishii K., Imanaka M., Nakayama H.** and **Kodama H.**, "Evaluation of the fatigue strength of adhesively bonded CFRP/metal single and single-step double-lap joints", *Compos sci technol,* (1999), **59**, 1675-1683.

5. **Curley A. J., Hadavinia H., Kinloch A. J.** and **Taylor A. C.**, "Predicting the service-life of adhesively-bonded joints", *Int. J. Fatigue*, (2000), **103**, 41-69.
6. **Krueger R., Paris I. L,** and **O'Brien T. K.**, "Fatigue life methodology for bonded composite skin/stringer configurations", *Proc. of the 15th ASC Technical Conference*, (2000), 729-736, Technomic Publishing, ISBN 1-58716-053-6.
7. **Bogy, D. B.** "Edge-bonded dissimilar orthogonal elastic wedges under normal and shear loading", *J Appl Mechanics,* (1968), **35**, 460-466.
8. **Lefebvre D. R.** and **Dillard D. A.**, "A stress singularity approach for the prediction of fatigue crack initiation in adhesive bonds. Part I: theory", *J Adhesion*, (1999), **70**, 119-138.
9. **Imanaka, M.**, **Ishii, K**., and **Nakayama, H.,** "Evaluation of fatigue strength of adhesively bonded single and single step double lap joints based on stress singularity parameters", *Eng Fract Mech*, (1999), **62**, 409-424.
10. **Sinclair, G. B., Okajima, M.** and **Griffin, J. H.** "Path independent integral for computing stress intensity at sharp notches in elastic strip", *Int J Numer Meth Engng*, (1984), **20,** 999-1008.
11. **Pradhan, S. C., Iyengar, N. G. R.** and **Kishore, N. N.** "Finite element analysis of crack growth in adhesively bonded joints", *Int J Adhes Adhes*, (1995), **15**, 33-41.
12. **Wahab, M. M. A. , Ashcroft, I. A., Crocombe, A. D.,** and **Shaw, S. J.** "Prediction of fatigue thresholds in adhesively bonded joints using mechanics and fracture mechanics", *J. Adhesion Sci. Technol.,* (2001), **15**/7, 763-781.
13. **Kayupov, M.** and **Dzenis, Y. A.** "Stress concentrations caused by bond cracks in single-lap adhesive composite joints", *Compos Struct*, (2001), **54**, 215-220.
14. **Quaresimin, M.**, "Fatigue of woven composite laminates under tensile and compressive loading" *Proceedings of 10th European Conference on Composite Materials* - ECCM10 Bruges - June 3-7, 2002.
15. **Lazzarin, P., Quaresimin, M.** and **Ferro, P.**, "A two-term stress function approach to evaluate stress distributions in bonded joints of different geometries", *J. Strain Anal Eng*, (2002), **37**/5, 385-398.
16. **Quaresimin, M., Ricotta, M.,** "Experimental analysis and fatigue life prediction of bonded composite joints", *Proceedings of XXXII AIAS* - September 3-6 2003 Salerno, Italy (in Italian).
17. **Rybicki, E. F., Kanninem, M. F.,** "A finite element calculation of stress intensity factors by a modified crack closure integral"**,** *Eng. Fract. Mech.*, **9** (1977), 931-938.
18. **Raju, I. S.,** "Calculation of strain energy release rates with higher order and singular finite elements", *Eng. Fract. Mech*, **28**/3 (1987), 251-274.
19. **Krueger, R., Minguet, P. J.,** and **O'Brien, T.K.,** "Implementation of interlaminar fracture mechanics in design: an overview", *Proceedings of ICCM14*, July 14-18 2003, San Diego, USA.